Talanta 85 (2011) 2437–2444

Contents lists available at ScienceDirect

Talanta

journal homepage: www.elsevier.com/locate/talanta

Using low frequency full bottle diamagnetic screening to study collectible wine

S.J. Harley, V. Lim, P.A. Stucky, M.P. Augustine*

Department of Chemistry, One Shields Avenue, University of California, Davis, CA 95616, United States

ARTICLE INFO

Article history:
Received 27 June 2011
Received in revised form 26 July 2011
Accepted 27 July 2011
Available online 5 August 2011

Keywords:
Diamagnetic
Wine
Principal component analysis
Counterfeit
Noninvasive

ABSTRACT

A low frequency $\nu < 30$ MHz spectrometer capable of noninvasively and nondestructively screening the diamagnetic properties of full intact bottles of wine is described, and along with principal component analysis, used to compare and contrast sealed bottles of wine. The sensitivity of this approach to various ionic and molecular wine solutes is established by analyzing standard solutions. The successful application of this full bottle method to a library of collectible wine is discussed and suggests that the method can be used to identify counterfeit wine without violating the bottle.

1. Introduction

Given that the value of collectible wine can easily approach several thousands of dollars (e.g. the 1985 Petrus Pomerol and the 1982 Chateau Latour are currently valued at $3500 and $2000 respectively [1]) and that high end wines are routinely counterfeited, it is interesting that the wine market has not demanded a method to verify wine authenticity without opening the bottle or violating the bottle seal. A bottle of wine is merely an opaque, often green, glass container housing a dark purple colored liquid that is labeled with a piece of paper having the wine maker mark; this is an easy target for counterfeiters. Whether an authentic empty bottle is backfilled with a lesser quality wine and carefully resealed or a lower grade sealed wine bottle is intentionally labeled with the mark of a higher quality wine, it is the ease of wine modifications and the absence of any available thwarting technology combined with the potentially large financial benefit that makes the selling of faux wines an attractive venture. The wine industry has attempted to stop counterfeiting by introducing high tech cosmetic changes to labels and corks [2–5]. Not only are these counter measures easily defeated, they do not address the fact that older bottles do not have these upgrades and that older bottles currently dominate the wine collection market. Unfortunately these efforts to defeat wine counterfeiters only increase the difficulty associated with marketing counterfeit wine as there is always a way to make an item appear externally authentic. A better approach is to compare the contents of the sealed suspected counterfeit wine bottle to the contents of accepted authentic sealed wine bottles of the same vintage and type. It is the unique flavor, texture, and aroma of wine produced by the specific combination of the numerous chemical constituents that not only makes consumption delightful but also indicates authenticity.

It is the complex wine making process that is responsible for every wine having specific chemical, element, or compound concentrations. The concentration variation of these compounds in wine is due to the viticultural and enological history of the wine or equivalently the details relating to grape growth, harvesting, storage, must extraction, fermentation, and bottling.

The viticultural based chemical compound concentration variability in wine is produced by both natural processes and external sources. Region specific soil conditions [6], the composition of available vineyard irrigation sources [7,8], and the climate [9] contribute to the various salt and ion concentrations in wine as both the quality and quantity of the harvest directly depend on how the grapes are grown. The sugar levels in mature grapes established during the growth process ultimately dictates the concentration of ethyl alcohol [10], glycerol [11], lactic acid [12], etc. following fermentation. These naturally induced chemical compound concentration variations in wine are further augmented by external mechanisms as well. Here environmental pollutants like lead or cadmium [13] can enter the plant if the vineyard is located near an urban environment or a major transportation corridor while sodium ion levels are known to be elevated in grapes obtained from vineyards exposed to ocean spray [14]. The application of fertilizers and pesticides to growing vines also modifies inorganic ion concentrations in wine. Fertilizers directly contribute to varying potassium, calcium, and phosphate concentrations [15] in wine

* Corresponding author. Tel.: +1 530 754 7550; fax: +1 530 752 8995.
E-mail addresses: augustin@chem.ucdavis.edu, maugust@ucdavis.edu (M.P. Augustine).

0039-9140/$ – see front matter © 2011 Elsevier B.V. All rights reserved.
doi:10.1016/j.talanta.2011.07.095

while pesticides can introduce cadmium, copper, manganese, lead, and zinc ions [16].

Inorganic and organic based chemical constituent concentrations in wine are also strongly affected by the enological processes applied following the grape harvest. It is well known that storage vessels, piping systems, and transfer containers increase aluminum, cadmium, chromium, copper, iron, and zinc ion concentrations [17]. Flocculants are often added to wine to improve clarity and remove particulate debris. This process further increases the sodium, calcium, or aluminum ion content in wine [18]. The application of pH buffering agents to stabilize wine acidity can add calcium or sodium carbonates to wine while preservation agents like sulfites are introduced to extend the wine lifetime [19]. The concentration of organic chemical compounds in wine is largely controlled by fermentation. For example, the length of the alcoholic fermentation period coupled with the type of yeast used and the naturally occurring grape sugar concentration dictates how much sugar is converted into alcohol [20]. In addition, glycerol formed during alcoholic fermentation may be subsidized with additional glycerol to control viscosity and perceived sweetness [11]. In a similar way the length of the malolactic fermentation period controls the percent conversion of malic acid to lactic acid [12]. Solid sedimentation on the bottom of stored wine bottles is another way that constituent levels may change. Interestingly the formation of bitartarate particulates in standing wine is acceptable to European standards yet it is considered objectionable by most Americans. Thus American wines are typically cold stabilized to crystallize and remove potassium bitartarate prior to bottling thus changing the bitartarate and potassium concentrations in wine [21].

At a concentration of 0.1–3 g/L potassium is the most prevalent ion in wine followed by sodium, calcium and magnesium [22]. It is variations in this high potassium concentration that are governed by soil conditions as mentioned above and the pronounced uptake of potassium by grape vines [23] that makes potassium an excellent geogenic marker. Although the concentration of the paramagnetic ions such as iron, copper, and manganese are substantially lower in wine (mg/L), these ions catalyze oxidative reactions that produce aldehydes, ketones, and carboxylic acids [24]. Thus while the concentration of catalytic amounts of these ions may not be directly quantifiable in sealed intact wine bottles, their effect on the concentration of other wine constituents may be determined.

There are numerous variables that impact the concentration of the inorganic and organic molecular constituents in bottled wine that reflect the viticultural and enological history of the final prepared wine. It is therefore unlikely that any two bottles produced from two different viticultural or enological processes would ever have the same chemical constituent concentrations or ionic and molecular fingerprint. Modern analytical chemistry approaches such as nuclear magnetic resonance (NMR) spectroscopy [25], gas chromatography/mass spectrometry (GC/MS) [26], light absorption [27], scattering [28], and elemental analysis [29] have been used to fingerprint wine. Here it has been shown that amino acid ratios [30], rare element abundance [31,32], or even deuterium quantification [33] afford region specific identification. However, as all of these approaches are invasive or destructive they are not directly applicable to valuable collectible wine. Collectors spending thousands of dollars for a single bottle realize that either opening the bottle or extracting small volumes of wine from the bottle immediately devalue the investment. It is for this reason that noninvasive wine constituent analysis was recently developed. Here high resolution NMR spectroscopy [25,34] and GC/MS [26] applied to full intact wine bottles was used to noninvasively and nondestructively screen bottled wine for oxidative spoilage mediated by leaky corks and for the presence of 2,4,6-trichloroanisole (TCA) or cork taint respectively. Although the NMR approach can monitor down to 100 mg/L acetic acid or acetaldehyde concentrations in wine, the use of full bottle NMR spectroscopy to screen for the lower concentration solutes that reflect wine origin and thus authenticity mentioned above is problematic due to sensitivity and resolution limitations. Here many of the ionic solutes contain non-NMR active or low natural abundance, low gyromagnetic ratio nuclei or are present at concentrations below the NMR detection threshold. The NMR spectra for the higher concentration molecular compounds such as ethyl alcohol, acetic acid, succinic acid, proline, and borate esters often spectrally overlap making identification difficult if not impossible in full intact wine bottles. The much higher sensitivity of the full bottle GC/MS approach is more attractive than NMR spectroscopy but the success enjoyed in the screening of bottle mounted corks for TCA does not apply to fingerprinting as just the outer surface of the cork is examined with this approach not the wine bottle contents.

More recently, low frequency radio waves were used to explore the dielectric response of intact wine bottles [35]. That approach used principal component analysis (PCA) to reduce the collected data into two wine specific data points, and the method described here uses the same basic strategy. Here the frequency dependent magnetic properties of wine in sealed intact bottles are probed by monitoring the effect of the frequency dependent magnetic susceptibility on the amplitude and phase of an applied oscillating magnetic field. The method combines the simple apparatus shown in Fig. 1 and the spectrometer shown in Fig. 2 with PCA [36] to

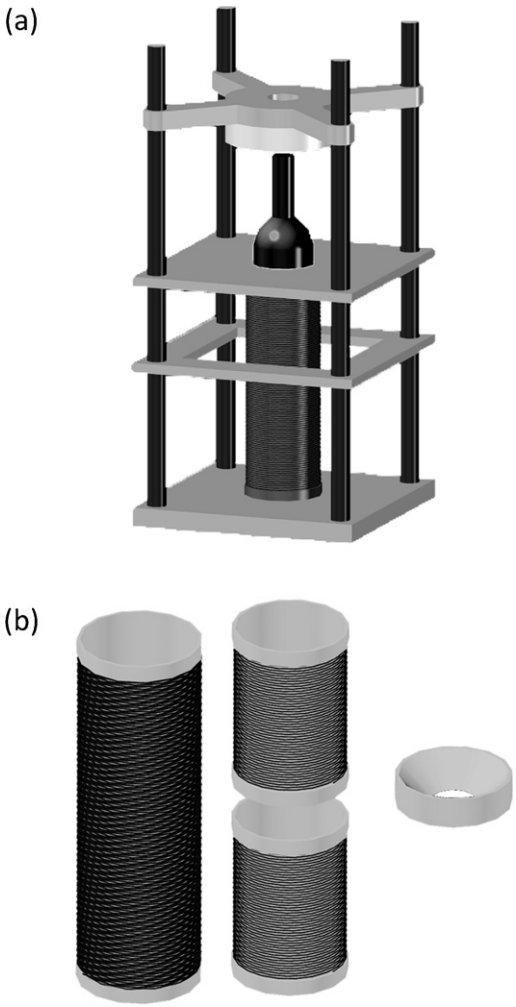

Fig. 1. Rendered image of the device used to monitor the induced magnetization of full intact wine bottles (a) and a separated view (b) showing the secondary coils along with the bottle holding insert.

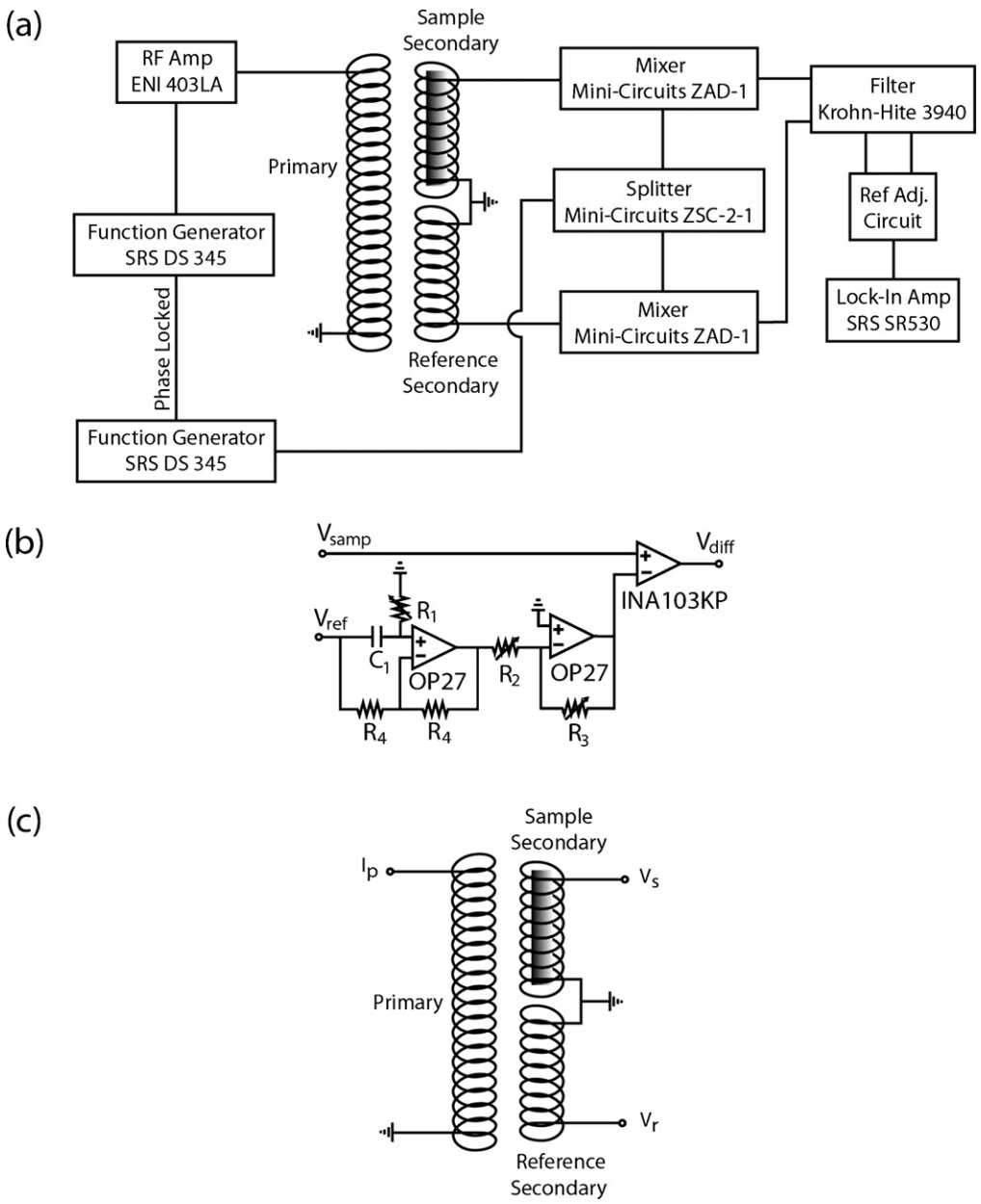

Fig. 2. (a) Schematic diagram of the device used to monitor the induced magnetization of full intact wine bottles. (b) Expanded view of the reference adjustment circuit. (c) Separate view of the primary solenoid and secondary show the sample and reference halves. The applied current I_p and induced voltages V_s and V_r are indicated.

compare same and different wine types, and vintages. Here a commercial off-the-shelf function generator broadcasts a frequency swept magnetic field across the wine bottle length via the primary solenoid shown in Fig. 1(a) as the outer coil directed along the long axis of the wine bottle, the left hand solenoid in Fig. 1(b), and the labeled primary in the spectrometer schematic shown in Fig. 2. The magnetic susceptibility of wine attenuates the amplitude and retards the phase of this applied magnetic field. These effects are monitored by the secondary coil that is mounted inside of the primary solenoid coil as shown in Fig. 1(b). One half of the secondary coil is labeled as the sample secondary and the other half serves as the reference secondary as shown in Fig. 2. Application of this method to several standard solutions of ethyl alcohol, acetic acid, potassium sulfate, and glycerol in deionized water with concentrations chosen to bracket the expected average concentration in wine suggests that different magnetic field frequencies can probe different constituents in wine. The frequency dependent magnetic field amplitude attenuation and phase retardation is not only reflected in the concentration of solutes specific to each wine but also in the total volume of the wine. The amplitude attenuation and phase retardation can be used in combination with PCA to group like wine vintages and essentially fingerprint wine. It is the comparison of a potential counterfeit bottle response to a known authentic wine that can be used to verify the contents of a suspected counterfeit bottle.

2. Theory

Direct magnetic field coupling between the primary and the sample secondary coils shown in Figs. 1 and 2 is the dominant source of induced voltage and therefore signal in the mutual inductor setup. Each half of the secondary coil is wound in the same direction. Connection of the midpoint of this coil to ground naturally limits any direct coupling signal from the primary coil. It is the

small perturbation to this direct coupling that is observed when a sample is added to one half of the secondary coil as shown in Fig. 2. The measured voltage V_s is strictly due to the induced magnetization of the sample or more specifically the complex magnetic susceptibility of the sample.

The voltage V_s measured from the sample secondary coil shown in Figs. 1 and 2 is related to the current applied to the primary coil I_p and more importantly to the magnetic susceptibility χ of the sample. In the case of an applied DC current I_p the applied magnetic field inside of the primary coil is

$$H = \frac{n_p I_p \pi r_p^2 b}{\ell_p} \tag{1}$$

where n_p is the number of turns in the primary coil, ℓ_p is the length of the primary coil, r_p is the radius of the primary coil, and b is an empirical correction factor. In the absence of any sample inside of the primary coil the magnetic induction B is

$$B = \mu_0 H \tag{2}$$

where the proportionality factor μ_0 is the permeability of free space. When a sample is placed inside of the primary coil described with a magnetic susceptibility χ the magnetization

$$M = \chi H \tag{3}$$

develops and adds to the applied magnetic field H to change the magnetic induction to

$$B = \mu_0(H + M) = \mu_0 H(1 + \chi) \tag{4}$$

In the case where paramagnetic substances are used $\chi > 0$ and an increase in the magnetic induction is observed while for diamagnetic samples the magnetic induction decreases as $\chi < 0$.

The steps leading to the result shown in Eq. (4) were included here as they directly apply to the actual experiment performed in this work. An oscillating current

$$I_p(t) = I_0 \ \cos(\omega t) \tag{5}$$

is applied to the primary coil giving

$$H(t) = H_0 \ \cos(\omega t) \tag{6}$$

since $H_0 = n_p I_0 \pi r_p^2 b/\ell_p$. As in the magnetostatic case shown in Eq. (2), in the absence of any sample, the applied time dependent field translates into the time dependent magnetic induction

$$B(t) = \mu_0 H_0 \ \cos(\omega t). \tag{7}$$

In parallel with an applied DC field, introduction of a sample to the primary coil leads to the creation of magnetization, however in the case of an applied oscillating field both an amplitude attenuation and a phase retardation of the applied time dependent field $H(t)$ is observed. The sample magnetization can be described as

$$M(t) = H_0[\chi'(\omega)\cos(\omega t) + \chi''(\omega)\sin(\omega t)] \tag{8}$$

where the in-phase dissipative and the quadrature dispersive frequency and sample dependent components of the magnetic susceptibility are given by $\chi'(\omega)$ and $\chi''(\omega)$ respectively. This equation can be used to rewrite the magnetic induction in Eq. (4) as

$$B(t) = H_0[(\mu_0 + \chi'(\omega))\cos(\omega t) + \chi''(\omega)\sin(\omega t)]. \tag{9}$$

It is the magnetic induction produced by the applied time dependent magnetic field $H(t)$ shown in Eq. (9) that leads to a measureable voltage V_s–V_r from the secondary coil shown in Fig. 2(c) that is mounted inside of the primary coil shown in Fig. 1(a). The sample voltage V_s is generated from the top half of the secondary coil containing the sample shown in Fig. 2(c) while the reference voltage V_r is produced from the sample-free lower half of the secondary coil shown in Fig. 2(c). In the absence of any sample in the optimum situation the primary coil produces the same field inside of both halves of the secondary coil yielding $V_s = V_r$ forcing the measured signal V_s–V_r to zero. This result, as well as the more applicable case where a sample is contained within the top half of the secondary coil with cross sectional area A_g and number of turns $n_g/2$, can be determined from Faraday's law of induction as

$$V_s = \frac{n_g}{2}\frac{d}{dt}\int \vec{B}(t)\cdot d\vec{A}$$

$$= \frac{n_g A_g H_0 \omega}{2}[(\mu_0 + \chi'(\omega))\sin(\omega t) - \chi''(\omega)\cos(\omega t)] \tag{10}$$

for the sample loaded half of the secondary coil and

$$V_r = \frac{n_g}{2}\frac{d}{dt}\int \vec{B}(t)\cdot d\vec{A} = \frac{n_g A_g H_0 \omega}{2}\mu_0 \sin(\omega t) \tag{11}$$

for the sample-free reference half of the secondary. The measured difference voltage

$$V_s - V_r = \frac{n_g A_g H_0 \omega}{2}(\chi'(\omega)\sin(\omega t) - \chi''(\omega)\cos(\omega t)) \tag{12}$$

naturally cancels the unwanted direct coupling effect between the primary and secondary coils because the ground point of the secondary coil is placed at the coil midpoint. Consequently the overall dynamic range dramatically improves and when the sample and reference halves of the secondary coil are perfectly balanced a background free experiment can be performed. Eq. (12) can be rewritten as

$$V_s - V_r = \frac{n_g A_g H_0 \omega}{2}\sqrt{\chi'(\omega)^2 + \chi''(\omega)^2}\cos\left[\omega t + \arctan\left(\frac{\chi''(\omega)}{\chi'(\omega)}\right)\right] \tag{13}$$

where the relationship between the measured amplitude

$$A(\omega) = \frac{n_g A_g H_0 \omega}{2}\sqrt{\chi'(\omega)^2 + \chi''(\omega)^2} \tag{14}$$

and phase

$$\phi(\omega) = \arctan\left(\frac{\chi''(\omega)}{\chi'(\omega)}\right) \tag{15}$$

to the material parameters $\chi'(\omega)$ and $\chi''(\omega)$ as a function of frequency ω can be used to establish a fingerprint for a particular sample.

3. Materials and methods

All chemicals were obtained from Sigma–Aldrich and used without further purification. Thirteen bottles of Charles Shaw wine obtained from Trader Joe's were drained, rinsed multiple times with water and acetone, and refilled with solutions of deionized water and ethyl alcohol, acetic acid, potassium sulfate, and glycerol. One bottle filled with deionized water served as a standard solution while the remaining twelve were filled with four sets of three solutions of each of these compounds as described in Table 1. The solution concentrations were chosen to bracket the average amounts reported for wine. Six sets of two duplicate bottles of collectible wine including the 1990 Grand Vin Chateau Latour, the 1958 Grand Vin Chateau Latour, the 2002 Opus One, the 1985 Opus One, the 1994 Petrus Pomerol, and the 1979 Petrus Pomerol were used to construct a wine authentication library. The spectrometer shown in Fig. 2(a) was used to measure the room temperature magnetic properties of the prepared full bottle solutions and the collectible wine in the 500 kHz < ν < 30 MHz frequency range in steps of 2 MHz. Here the output of a Stanford Research Systems SRS DS345 function generator was sent into an ENI 403LA 3 Watt RF amplifier whose output I_p was then used to drive the primary coil. The 9.8 cm diameter × 26.7 cm long primary coil is a solenoid with one layer of tightly packed 1.29 mm diameter enameled, copper

Table 1
Model solution sample set with estimated sensitivity.

Solute	Concentration			Sensitivity
	Sample 1	Sample 2	Sample 3	
Ethyl alcohol	20.00 ± 0.01% (v/v)	13.00 ± 0.01% (v/v)	5.00 ± 0.01% (v/v)	0.93 ± 0.02
Acetic acid	3.75 ± 0.05 mL/L	2.25 ± 0.05 mL/L	0.375 ± 0.05 mL/L	20.74 ± 0.15
Potassium sulfate	2.39 ± 0.01 g/L	0.747 ± 0.01 g/L	0.253 ± 0.01 g/L	65.51 ± 0.08
Glycerol	19.78 ± 0.01 g/L	10.00 ± 0.01 g/L	4.02 ± 0.01 g/L	0.75 ± 0.01

magnet wire. The secondary coil is comprised of two solenoids connected in parallel. Each 9.2 cm diameter × 12.7 cm long solenoid coil contains two layers of tightly wrapped 1.29 mm diameter enameled, copper magnet wire.

The voltages induced in the top half V_s and bottom half V_r of the secondary coil are directed into Minicircuits ZAD-1 mixers whose local oscillator port is driven by the output of a Minicircuits ZSC-2-1 split second phase locked SRS DS345 operating 1 kHz lower in frequency. The intermediate frequency outputs of the mixers were directed into a Krohn-Hite 3940 operating as a low pass filter with 20 dB of gain on each channel. This filtering/gain step effectively removes the difference frequency and enhances signal strength. The output channel of the Krohn-Hite 3940 corresponding to the sample voltage V_s is directed into one port of an INA 103KP instrumentation amplifier while the other output channel of the Krohn-Hite 3940 corresponding to the reference voltage V_r is directed into an Analog Devices OP27EZP configured as an all-pass filter and then another Analog Devices OP27EZP configured as an inverting gain amplifier prior to being inserted into the other INA 103KP instrumentation amplifier port. This configuration of the detection electronics allows the dynamic range of the measurement to be dramatically improved by adjusting the OP27EZP R1, R2, R3, and R4 resistors, shown in Fig. 2(b), to null the V_s–V_r signal for a standard sample of deionized water at each frequency prior to the measurement of real full bottle samples at that frequency. Operation in this way effectively background subtracts the effects of both the container and solvent on the measured signal leaving only contributions from the remainder of the wine solutes. The amplitude and phase of the difference signal from the output of the instrumentation amplifier corresponding to the V_s–V_r signal is then measured with a Stanford Research Systems SRS530 lock-in amplifier. A third phase locked Stanford Research Systems DS345 was used as a reference for the lock-in amplifier. All measurements were accomplished at room temperature, 20 °C. All of the data was mean centered prior to the application of PCA using MATLAB.

4. Results

The diamagnetic response for each of the samples shown in Table 1 was obtained in the 500 kHz < ν < 30 MHz frequency range using the apparatus shown in Figs. 1 and 2 as described in Section 3. The amplitude attenuation and phase retardation of the input stepped frequency input due to diamagnetic absorption for the three separate solution concentrations for each solute was used to construct a sample library. In this way four separate three sample libraries were created to demonstrate the solution dependence of the dielectric absorption of specific wine constituents. The right hand column in Table 1 corresponds to the sensitivity of the method to expected natural solute concentrations, a number that is determined from the slope of the PC_1 score or projection of the measured amplitude attenuation and phase retardation values for a given solute concentration onto the first principal component $\overrightarrow{PC1}$ for the entire solute concentration library. The diamagnetic responses for the twelve collectible wines were obtained in the 500 kHz < ν < 30 MHz frequency range in 2 MHz steps as described in Section 3. The amplitude attenuation and phase retardation at each frequency for each bottle was used to construct a library. Principal component analysis followed by projection of the amplitude attenuation and phase retardation data for a given bottle onto the first two principal components yields the PC_1 and PC_2 scores for each bottle shown in the plot in Fig. 3. Here the closed and open squares correspond to the PC_1, PC_2 scores for the 1985 and the 2002 vintages of Opus One respectively, the closed and open lozenges correspond to the PC_1, PC_2 scores for the 1958 and 1990 vintages of Grand Vin Chateau Latour respectively, and the closed and open triangles correspond to the PC_1, PC_2 scores for the 1979 and 1994 vintages of Petrus Pomerol respectively. In this case, the percentage of the total variance captured by projecting the measured data onto the first two principal components is more than 97%.

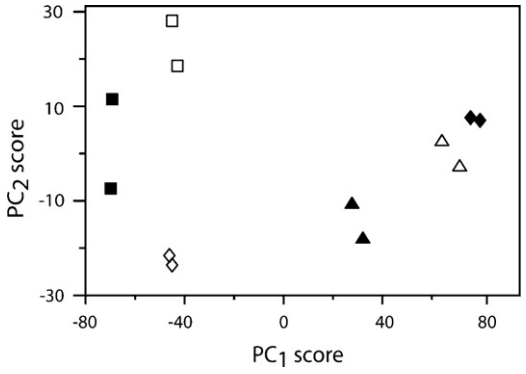

Fig. 3. PC_1 and PC_2 scores plot for the twelve bottle collectible wine library. The closed and open squares correspond to the 1985 and the 2002 vintages of Opus One respectively, the closed and open lozenges correspond to the 1958 and 1990 vintages of Grand Vin Chateau Latour respectively, and the closed and open triangles correspond to the 1979 and 1994 vintages of Petrus Pomerol respectively.

5. Discussion

It is important to begin this section by mentioning that the spectrometer shown in Fig. 2 operates in zero-background mode by electronically balancing the secondary coil at each frequency by forcing the SRS530 lock-in output voltage to <50 μV when the sample half of the secondary coil is loaded with a wine bottle filled with deionized water. The following three observations confirm that the signals reported here are wine dependent. First, the addition of wine solutes to the water standard sample at concentrations typically found in wine generate approximately 1 V output signals from the SRS530 lock-in amplifier at all input frequencies. Second, the removal of solution from the standard bottle generated much larger output voltages that saturated the lock-in amplifier. Third, the use of other wine bottles filled with deionized water generated signals much less than the characteristic 1 V wine dependent output signals. This final observation relates to the origin of and the geometry dependence of the magnetic susceptibility measurements. Subtle bottle-to-bottle glass composition changes appear to have little effect on the measurements presumably because the magnetism at the low frequencies used here is mediated by charge flow, an effect that dominates the static susceptibility offered by

the glass constituents. The geometry dependence of the measurements reported here is also of little concern. The coil arrangement shown in Fig. 2 is specific for either Bordeaux or Burgundy style bottles and the coils are arranged to monitor signals from the largest diameter part of the wine bottle. The cylindrical symmetry of the measurement volume is conserved in all cases and the only bottle-to-bottle variable is diameter. The amount of added or subtracted wine due to this diameter variation is small and is an extremely minor perturbation to the overall signal. Even if the bottle geometry dominated the observed signal, there would still be no issue from the point of view of counterfeit wine detection. Typically a given rare, collectible wine vintage is always stored in the same style bottle, obtained from the same manufacturer, and from the same lot.

The spectrometer shown in Fig. 2 generates wine dependent responses since replacement of the standard water sample with full intact bottles of wine led to output signals with wine specific phases and approximately 1 V amplitudes. The spectrometer shown in Fig. 2 was constructed with the intent of studying wine and the predominant goal of the device is to amplify subtle magnetic field amplitude and phase changes due to the frequency dependent magnetic susceptibility of wine. An alternative approach would involve coupling the primary solenoid coil shown in Fig. 1(a) and Fig. 2 to a vector impedance meter, LCR meter, or network analyzer to monitor the complex wine and frequency dependent magnetic susceptibility. Unfortunately such an approach does not offer enough bottle-to-bottle amplitude and phase dynamic range and sensitivity to separate different wines. It is the zero-background approach established by nulling the output signal from the SRS530 lock-in at each frequency to <50 μV for the water bottle standard combined with the narrow-banding and amplification characteristics provided by heterodyne detection and lock-in amplification that provides an output voltage amplitude and phase sensitivity appropriate for screening collectible wine. Although the use of feedback along with the instrumentation amplifier to balance the secondary coil in the spectrometer shown in Fig. 2 is specialized, every component in this circuit and the remainder of the spectrometer with the exception of the primary solenoid and secondary coil are commercial off-the-shelf items. The guiding principal in the primary and secondary coil design was wine bottle shape and size and the fact that more coil turns typically increase the coupling of the coils to the sample and thus measured signal strength. However, such a design approach has two limitations. Here the complex impedance of a wine bottle size solenoid inductor coupled to a similar size secondary make it difficult to uniformly couple RF energy into the wine bottle at each frequency. Consequently frequencies corresponding to low impedance regions of the coil are used to minimize reflected RF power and maximize RF coupling into and out of the wine bottle. A second problem with using as many coil turns as possible in the primary and secondary inductor designs is the inability to probe the extremely low <500 kHz portion of the frequency dependent magnetic susceptibility. Given these two issues, further gains in instrument sensitivity and flexibility could be achieved by optimizing instrument bandwidth and sensitivity as a function of primary solenoid and secondary coil shape, size and respective numbers of turns. However, as the current coil configuration regularly permits secondary coil balancing to the <50 μV level for water and approximately 1 V signals are observed following lock-in amplification such an effort was not pursued.

The steady state theory described in Section 2 suggests that it is the frequency dependent magnetic susceptibility $\chi'(\omega)$ and $\chi''(\omega)$ as a function of frequency ω calculated from the measured frequency dependent amplitude and phase that is used to establish a wine fingerprint for comparison to other wines. Such a calculation is never accomplished as it is the raw voltage amplitudes and phases that are used as input for PCA not calculated $\chi'(\omega)$ and $\chi''(\omega)$ values. This wine screening method is then an empirical, macroscopic approach rather than the analytical, microscopic techniques often used to study the molecular structure of pure liquids and simple mixtures. In other words, the theory described in Section 2 is specific for an ideal nonrealistic case where perfectly homogeneous magnetic fields are present and the solenoid and secondary coils are perfectly matched to yield zero output signal in the absence of any sample in either leg of the secondary coil. Since in practice the solenoid and secondary coil are not perfectly balanced the true experimental situation is far from ideal and calculation of $\chi'(\omega)$ and $\chi''(\omega)$ from Eqs. (14) and (15) derived for the perfect ideal case where physical characteristics of the coaxial inductors are largely absent is not practical. Furthermore, the measured voltage amplitudes and phases from the SRS530 lock-in amplifier are obtained in zero background mode as the signal for a standard water bottle sample is nulled to <50 μV prior to measurement of full intact wine bottles. The actual measured amplitudes and phases for wine from the spectrometer shown in Fig. 2 are therefore indirectly related to $\chi'(\omega)$ and $\chi''(\omega)$ at best. It is likely that the actual $\chi'(\omega)$ and $\chi''(\omega)$ values for wine would not be any more useful towards fingerprinting than raw voltage amplitudes and phases as wine is a complex mixture of organic and inorganic molecules and ions that all contribute to $\chi'(\omega)$ and $\chi''(\omega)$. Thus even if $\chi'(\omega)$ and $\chi''(\omega)$ were carefully determined it is unlikely that any theory would be able to reliably predict the experimental values. The purpose of Section 2 is therefore to not provide a bridge between microscopic chemical structure dependent parameters and macroscopic observables but to describe the origin of the wine dependent voltage amplitude and phase differences monitored by the spectrometer shown in Fig. 2(a).

The magnetic susceptibility at the low frequencies used in this study captures the interaction of the applied time dependent magnetic field with the nuclear, molecular, and unpaired electron magnetic moments in wine and since wine is a salt solution the diffusing charge experiences a Lorentz force. It is the eddy currents established by the primary solenoid coil and mediated by the Lorentz force and wine viscosity that likely lead to the effects reported here. As the Lorentz force dominates the Zeeman interaction at these low frequencies, solutions or wines with low mass highly charged ions will support the formation of larger eddy currents leading to larger values of $\chi'(\omega)$ and $\chi''(\omega)$ and ultimately producing larger measurable signals. The model solution library shown in Table 1 supports these comments. Here three separate solutions of ethyl alcohol, acetic acid, potassium sulfate, and glycerol in water with concentrations chosen to bracket the appropriate concentration in wine were prepared and studied with the spectrometer shown in Fig. 2. The zero background voltage amplitudes and phases at fifteen frequencies between 2 and 30 MHz yields (3 samples) × (15 measurements/sample) × (2 amplitude and phase points/measurement) × (1 library point/amplitude and phase point) = 90 library data points per solute library. These 90 library data points are subjected to PCA and each of the raw (15 measurements/sample) × (2 amplitude and phase points/measurement) = 30 amplitude and phase points/sample were projected onto the first principal component $\overrightarrow{PC\,1}$. The slope of these PC_1 scores as a function of solute concentration yields the sensitivity estimate shown in the right hand column in Table 1. The sensitivity ordering in Table 1 as potassium sulfate, acetic acid, ethyl alcohol, and glycerol is consistent with eddy currents being the primary contribution to $\chi'(\omega)$ and $\chi''(\omega)$. Here potassium sulfate completely ionizes in water leading to the greatest sensitivity, acetic acid partially dissociates yielding an intermediate sensitivity, and the small molecular hydroxide species ethyl alcohol and glycerol have the lowest sensitivity. The origin of the small sensitivity difference between ethyl alcohol and glycerol could be due to the higher concentration of the ethyl alcohol solutions in

comparison to the glycerol solutions, the lower mass of ethyl alcohol in comparison to glycerol, or some material properties of the ethyl alcohol and glycerol solutions like the presence of a dynamic glass transition [37]. It is important to note that other test solutions have been studied with this approach that are not reported here. For example, the method is not sensitive to sucrose solutions in water with concentrations similar to that known for wine. This solution set in addition to other molecular/water solution sets is consistent with the expected frequency dependence of the magnetic susceptibility. The magnetic response of larger molecular compounds like sugars, flavenoids, and tannins tends to be in the microwave region, at frequencies two orders of magnitude higher than the 30 MHz maximum frequency used here. However, because of the difficulty in coupling microwave magnetic energy into a standard wine bottle and the acceptable sensitivity observed at lower frequency, higher frequencies were not explored here.

The sensitivity of this diamagnetic screening approach to specific wine solutes at concentrations appropriate for native wine prompted the application to a rare wine library. Here six vintages with two bottles/vintage comprised a 12 sample rare wine library. Again voltage amplitudes and phases for each sample were obtained at 15 different frequencies leading to a (12 samples) × (15 measurements/sample) × (2 amplitude and phase points/measurement) × (1 library point/amplitude and phase point) = 360 amplitude and phase point data set that was subjected to PCA. Since more than 97% of the library variance was contained in the first two principal components $\overrightarrow{PC\,1}$ and $\overrightarrow{PC\,2}$, a plot of the PC_1 and PC_2 scores for measured data for each of the 12 samples captures more than 97% of the magnetic susceptibility variance in the measured data and reduces the dataset dimensionality from 360 to 2. The plot shown in Fig. 3 summarizes these PC_1, PC_2 scores where the closed and open squares correspond to the 1985 and the 2002 vintages of Opus One, respectively, the closed and open lozenges correspond to the 1958 and 1990 vintages of Grand Vin Latour, respectively, and the closed and open triangles correspond to the 1979 and 1994 vintages of Petrus Pomerol, respectively. With the exception of the two bottles of the 1985 Petrus Pomerol labeled as closed squares in Fig. 3, the proximity of the PC_1, PC_2 scores to each other confirms that the contents of identical sealed, labeled bottles is the same. Addtionally, the separation of the PC_1, PC_2 scores from each other that suggests that the contents of differently sealed, labeled bottles are in fact different.

The largest separation between like wines in Fig. 3 corresponds to the closed squares or the 1985 Petrus Pomerol. This is a real difference, as re-investigation of a randomly chosen sample from the rare wine library (1990 Latour) on a different day at precisely the same temperature yielded a data point lying exactly on top of the appropriate data point shown in Fig. 3. The origin of this difference could be that one of the two 1985 Petrus Pomerol bottles is a counterfeit, spoiled, or heat damaged. These observations and possibilities are consistent with dielectric measurements on the same two 1985 Petrus Pomerol bottles reported elsewhere [35]. A similar large difference between the two PC_1, PC_2 scores for these samples was recognized in that study as well and attributed to one or all of these mechanisms. Investigation of a larger representative sample set for the 1985 Petrus Pomerol, a study extremely limited by rare wine availability, would provide more insight into which of the two 1985 Petrus Pomerol bottles is an outlier. In the absence of planned future studies that empirically relate specific wine solutes that reflect spoilage, improper storage, or other wine related phenomena to the statistical parameters measured with this approach, both the suspect wine bottle and a representative authentic wine bottle would have to be violated or opened to determine the reason for the difference between the two points shown in Fig. 3. However, if one is only interested in whether a particular bottle contains the appropriate wine, this approach provides a way to compare the bottle to an accepted collection of authentic wines. It is the similarity between points on the PC_1, PC_2 scores plot for suspect and authentic bottles of sealed wine that can be exploited to detect counterfeit wines without opening the bottle or violating the bottle seal.

6. Conclusion

A spectrometer capable of monitoring electrical signals that are proportional to the frequency dependent magnetic susceptibility of wine in sealed intact bottles was described and used to compare the same and different wine vintages. The empirical performance of the instrument on sealed bottles was demonstrated by applying the method to a model solution set prepared with major wine solutes at expected wine concentrations. The sensitivity of this approach to ethyl alcohol and other molecular solutes and salts prompted the investigation of a rare wine library. It is the combination of a low frequency magnetic method capable of noninvasively probing wine in sealed bottles with the machinery of PCA and access to a true rare wine library where an intimate knowledge of the wine bottle history is known that not only motivated this study but also contributed to the success of the work. The method has the potential to identify counterfeit wines as long as measurements on the suspect bottle are compared to those for known authentic bottles. Thus, access to a vast rare wine collection with known authentic wines is required to realize the usefulness of the approach as the method in its current form, much like any fingerprinting approach, cannot determine the authenticity of wine without known authentic standards.

The work presented here is just one application of the overriding idea that uses PCA to establish empirical relationships between an abundance of data and a collection of samples. This study used a test sample set to demonstrate that the method is sensitive to native solute concentrations in wine. The approach was then applied to a small library of rare collectible wine. A future direction involves investigation of the statistical nature of the PC_1, PC_2 score clustering shown in Fig. 3. Here access to many bottles of the same vintage with known histories will be used to develop confidence limits for the identification of counterfeit wines; that information is not possible to determine from the two data points for each wine shown in Table 1. A second study addresses other potential problems noticed in rare collectible wine other than the detection of potential counterfeits. For example, the principal components for the molecular solutes ethyl alcohol and glycerol can have the opposite sign as the same principal components for the ionic solutes potassium sulfate and acetic acid. In addition, it was noticed in a previous dielectric study [35] that the first principal component values at certain frequencies increase and others decrease as a function of time after a wine bottle has been opened. These particular frequencies correspond to the maximum variation of the first principal components appropriate for ethyl alcohol and acetic acid. A similar measurement using the diamagnetic approach presented here is currently underway. The future of this work is rich with possibilities including the study of the empirical effects of wine storage, aging, heat damage, etc. in collectible rare wine without opening the bottle.

Acknowledgement

A steady supply of collectible rare wine from Gene Mulvihill is gratefully acknowledged.

References

[1] C. Deverell, Molecular Physics An International Journal at the Interface Between Chemistry and Physics 18 (1970) 319–325.
[2] A. Afzali-Ardakani, C. Feger, M. Martens, P. Moskowitz, A. Schrott, C. Tresser, Method and Systems for Preventing Parallel Marketing of Wholesale and Retail Items, Patent Appl. No. US 2002/0143671 A1 (2002).

[3] http://www.anl.gov/Media_Center/News/2008/NE080801.html, 2011.
[4] Business Wire, Kodak Helps Napa Valley Wineries Fight Wine Fraud, 2007.
[5] De La Rue International, Case Study Brand Authentication for Romanian Wine, 2007.
[6] D.I. Jackson, P.B. Lombard, American Journal of Enology an Viticulture 44 (1993) 409–430.
[7] W.J. Hardie, J.A. Considine, American Journal of Enology an Viticulture 27 (1976) 55–61.
[8] Y. Hepner, B. Bravdo, American Journal of Enology an Viticulture 36 (1985) 140–147.
[9] G.V. Jones, R.E. Davis, American Journal of Enology an Viticulture 51 (2000) 249–261.
[10] E.A. Crowell, C.S. Ough, American Journal of Enology and Viticulture 30 (1978) 61–64.
[11] A.C. Noble, G.F. Bursick, American Journal of Enology and Viticulture 35 (1984).
[12] D. Wibowo, R. Eschenbruch, C.R. Davis, G.H. Fleet, T.H. Lee, American Journal of Enology and Viticulture 36 (1985) 302–313.
[13] S. Galani-Nikolakai, N. Kallithrakas-Kontos, A.A. Katsanos, Science of the Total Environment 285 (2002) 155.
[14] M.A. Amerine, G. Thoukis, R.V. Marfa, American Journal of Enology and Viticulture 4 (1953) 157–166.
[15] C. Diaz, J.E. Conde, S.J. Estevez, P. Olivero, P. Perez Trujillo, Journal of Agricultural and Food Chemistry 51 (2003) 4303–4308.
[16] F. Nasir, A.G. Jiries, M.I. Batarseh, F. Beese, Environmental Monitoring and Assessment 66 (2001) 25–263.
[17] P. Kment, M. Mihaljevic, V. Ettler, O. Sebek, L. Strnad, L. Rohlova, Food Chemistry 91 (2005) 157–166.
[18] B.W. Zoecklein, K.C. Fugelsang, B.H. Gump, F.S. Nury, Wine Analysis and Production, Springer, 1995.
[19] M. Alvarez, I.M. Moreno, M.A. Jos, A.M. Camean, A.G. Gonzalez, Journal of Food Composition Analysis 20 (2007) 391–395.
[20] G.H. Fleet, Wine: Microbiology and Biotechnology, Taylor and Francis, London, 2002.
[21] J.H. Fessler, Process of Cold Stabilization of Wine, Patent Appl. No. 770,852 (1978).
[22] P. Pohl, Trends in Analytical Chemistry 26 (2007) 941–949.
[23] C.G. Dundon, R.E. Smart, M.G. McCarthy, American Journal of Enology an Viticulture 35 (1984) 200–205.
[24] S.R. Mozaz, A.G. Sotro, J.G. Segovia, C.A. Azpilicueta, Food Research International 32 (1999) 683–689.
[25] A.J. Weekley, P. Briuns, M. Sisto, M.P. Augustine, Journal of Magnetic Resonance 161 (2003) 91–98.
[26] V. Lim, S. Harley, M.P. Augustine, American Journal of Enology and Viticulture (2011) doi:10.5344/ajev.2011.10106.
[27] D. Cozzolino, Non-Destructive Analysis by VIS-NIR Spectroscopy of Fluid(s) in its original container, Patent Appl. No. AU 2005100565 A4 (2005).
[28] C. Eliasson, N.A. Macleod, P. Matousek, Analytica Chimica Acta 607 (2008) 50–53.
[29] P. Serapinas, P.R. Venskutonis, V. Aninkevicius, Z. Ezerinkskis, A. Galdikas, V. Juzikiene, Analytical Methods 107 (2008) 1652–1660.
[30] A. Carpentieri, M. Gennaro, A. Amoresano, Analytical and Bioanalytical Chemsitry 389 (2007) 969–982.
[31] O. Lutz, Naturwissenschaften 78 (1991) 67–69.
[32] J.D. Greenough, H.P. Jackson, H.P. Longerich, Australian Journal of Grape and Wine Research (1997) 75–83.
[33] G.J. Martin, C. Guillou, M.L. Martin, M.T. Cabanis, Y. Tep, J. Aerny, Journal of Agricultural and Food Chemistry 36 (1988) 316–322.
[34] A.J. Weekley, P. Briuns, M.P. Augustine, Journal of Enology and Viticulture 53 (2003) 18–3214.
[35] S.J. Harley, V. Lim, M.P. Augustine, Analytica Chimica Acta 702 (2011) 188–194.
[36] I.I. Jolliffe, Principal Component Analysis, 2nd ed., Springer, Berlin, 2002.
[37] A. Puzenko, Y. Hayashi, Y. Ryabov, I. Balin, Y. Feldman, U. Kaatze, R. Behrends, Journal of Phyiscal Chemistry 109 (2005) 6031–6035.